FORMATION OF LARGE REGULAR SATELLITES OF GIANT PLANETS IN AN EXTENDED GASEOUS NEBULA II: SATELLITE MIGRATION AND SURVIVAL. I. Mosqueira, *NASA Ames Research Center/SETI, Moffett Field CA 94035, USA (mosqueir@cosmic.arc.nasa.gov)*, P. R. Estrada, *Cornell University, Ithaca CA 14853, USA, (estrada@astro.cornell.edu).*

Using an optically thick inner disk and an extended, optically thin outer disk as described in Mosqueira and Estrada (2002), we compute the torque as a function of position in the subnebula, and show that although the torque exerted on the satellite is generally negative, which leads to inward migration as expected (Ward 1997), there are regions of the disk where the torque is positive. For our model these regions of positive torque correspond roughly to the locations of Callisto and Iapetus. Though the outer location of zero torque depends on the (unknown) size of the transition region between the inner and outer disks, the result that Saturn's is found much farther out (at $\sim 3r_c^S$, where r_c^S is Saturn's centrifugal radius) than Jupiter's (at $\sim 2r_c^J$, where r_c^J is Jupiter's centrifugal radius) is mostly due to Saturn's less massive outer disk, and larger Hill radius.

For a satellite to survive in the disk the timescale of satellite migration must be longer than the timescale for gas dissipation. For large satellites (~ 1000 km) migration is dominated by the gas torque. We consider the possibility that the feedback reaction of the gas disk caused by the redistribution of gas surface density around satellites with masses larger than the inertial mass (Ward 1997) causes a large drop in the drift velocity of such objects, thus improving the likelihood that they will be left stranded following gas dissipation. We adapt the inviscid inertial mass criterion to include gas drag, and m-dependent non-local deposition of angular momentum.

We find that such a model holds promise of explaining the survival of satellites in the subnebula, the mass versus distance relationship apparent in the Saturnian and Uranian satellite systems, and the observation that the satellites of Jupiter get rockier closer to the planet whereas those of Saturn become increasingly icy. It is also possible that *close* to the planet micron-sized dust production keeps the gas disk optically thick, leading to weak gas turbulence that removes gas on the same timescale as the orbital decay time of midsized ($200 - 700$ km) regular satellites located inside the centrifugal radius of the primary. Either way, we argue that Saturn's satellite system bridges the gap between those of Jupiter and Uranus by combining the formation of a Galilean size satellite in an optically thick subnebula with a strong temperature gradient, and the formation of smaller satellites, close to the planet, in a cool gas disk with optical depth ~ 1, and a weak temperature gradient. Our model also provides an explanation for the presence of regular satellites outside the centrifugal radii of Jupiter and Saturn, and the absence of such a satellite for Uranus.

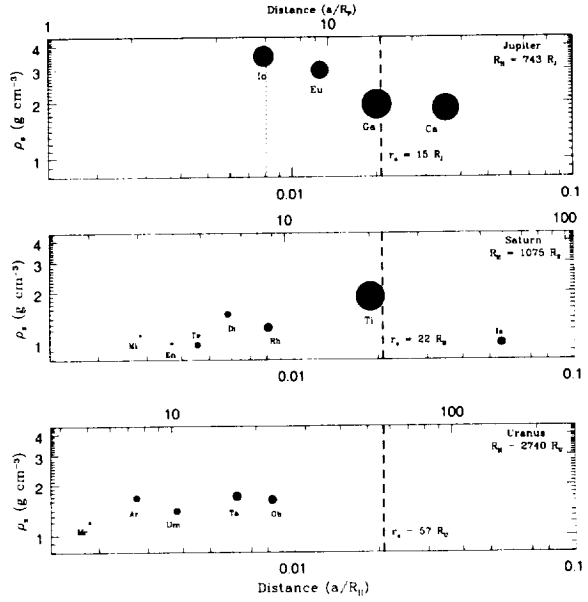

Figure 1: A comparison of the three giant planet satellite systems under consideration in this study. Here we plot the known densities of the satellites as a function of distance from the planet in units of their respective primary's Hill radius. The centrifugal radius $\sim R_H/48$ is denoted by a bold dashed line. The dotted line at roughly $\sim R_H/100$ corresponds to the innermost portion of the disk.

1 Introduction

As discussed in Mosqueira and Estrada (2002, submitted to Icarus, hereafter Paper I), considering gas opacity only, our subnebula model has an optically thick inner disk inside the centrifugal radius, and an optically thin outer disk. In Paper I we adopted a turbulence model along the lines of the scenario envisioned by Klahr and Bodenheimer (2001, in press). Such a model leads to turbulence that is a function of position and time. In particular, nearly isothermal regions of the disk would be largely quiescent and laminar. Because the inner disk is expected to be non-isothermal both radially and vertically, this region of the disk should remain weakly turbulent and viscous at least as long as it remains optically thick.

Nevertheless, gas is not easy to get rid of. As stated, a constant viscosity model may not apply. In Paper I we argued that dust opacity is unlikely to be sufficient to keep the gas disk optically thick (although the possibility cannot be ruled out). At least for low optical depth isothermal disks a quiescent gas disk is more plausible. Such a disk would be characterized by weak viscosity and very long evolution times. As a result, it

is unclear how one can remove this gas in a short timescale. Furthermore, recent work suggests that the process of gap opening does not completely shut-off the accretion of gas onto the planet (Lubow *et al.* 1999). If so, one would expect gas in the subnebula for as long as there was gas in the nebula itself, $\sim 10^7$ years, when it is expected to dissipate due to photodissociation and solar wind.

TABLE I
Satellite Data[a]

	Distance (R_P)	Radius (km)	Density (g cm^{-3})	Mass (10^{26} g)
Jupiter	1.0	71492	1.326	18980
Io	5.905	1,821	3.53	0.894
Europa	9.937	1,565	2.97	0.480
Ganymede	14.99	2,634	1.94	1.4823
Callisto	26.37	2,403	1.85	1.0776
Saturn	1.0	60330	0.687	5684.6
Mimas	3.075	199	1.12	0.00037
Enceladus	3.945	249	1.00	0.00065
Tethys	4.884	529	0.98	0.0061
Dione	6.256	560	1.49	0.011
Rhea	8.736	764	1.24	0.023
Titan	20.25	2,575	1.88	1.3457
Iapetus	59.03	720	1.0	0.016
Uranus	1.0	25559	1.318	868.32
Miranda	5.08	240x233	1.20	0.000659
Ariel	7.48	581x578	1.67	0.0135
Umbriel	10.4	585	1.4	0.0117
Titania	17.05	790	1.71	0.0353
Oberon	22.8	760	1.63	0.0301

[a] From *TheNewSolarSystem*, J. K. Beatty, Ed. (1999)

In terms of the satellite system observations, the presence of gas might be desirable to clear up debris, damp eccentricities and inclinations (especially in the case of Uranus where the axis is tilted), provide size dependent sorting (observed in the Saturnian and Uranian satellite systems), and as a selective loss mechanism of silicates (inside Titan, the Saturnian satellite system is mostly made of ice). Also, the capture of the irregular satellites would seem to favor the presence of gas in the system not only for capture into planetary orbits (Pollack *et al.* 1979), but also for capture into resonance. Indeed it is likely that these objects required strong gas drag for planetary capture followed by weak gas drag for resonance capture (Saha and Tremaine 1993). In Saturn's system, the capture of Hyperion into a 4:3 mean motion resonance with Titan poses problems given the weakness of the tidal forces on Titan. Tidal capture would require too low a coefficient of dissipation Q of Saturn given the proximity of Mimas to the planet. Recently Lee and Peale (2000) suggested that Hyperion was captured into resonance by proto-Titan in the presence of a strong gas surface density gradient.

It is also tantalizing to assume that the sizes of the satellites are somehow connected with the gap opening criterion, and the positions of of the satellites are connected with the size of gas disk around the protoplanet. We can obtain an estimate of the size of this disk by the centrifugal radius of the planet (*e.g.* Stevenson *et al.* 1986), which assumes that gas elements conserve specific angular momentum once they enter the planet's Hill sphere. One must keep in mind, however, that Callisto and Iapetus are well outside the centrifugal radius of Jupiter and Saturn respectively. Finally, as discussed in Paper I, the ratio of masses of the atmospheric envelopes (using core masses of about fifteen Earth masses for both planets) of Jupiter to Saturn is similar to the ratio of mass in the reconstituted Galilean satellites to the mass in the Saturnian satellite system of ~ 3.7. Furthermore, the atmospheric envelope ratio between Saturn and Uranus is ~ 18 (assuming a ten Earth core mass for Uranus), which is also similar to the ratio of mass in their respective satellite systems (~ 15). This may indicate that the amount of material left to make the satellite systems was directly related to the amount of gas in the giant planet envelope. This strongly suggests that the formation of the satellite systems has to be placed in the context of the planetary subnebula that led to them.

The issue of survival in the presence of gas affects objects of all sizes. Small objects will migrate inwards due to gas drag (Weidenschilling 1984). Larger objects will generally migrate inwards as a result of gas tidal torque (Ward 1997). Hence we are led to consider how satellites may survive in the presence of gas long enough for gas dissipation to take place.

In section 2 we discuss the regular satellites of giant planets and advance the general framework that will be the focus of this paper. In section 3 we compute the gas tidal torque as a function of position in the inner and outer Jovian disks. In section 4 we discuss Galilean satellite gap opening, migration and survival. In section 5 we discuss how our model applies to Saturn's satellite system. In section 6 we extend the model to Uranus. In section 7 we present our summary and discussion.

2 Regular Satellites of Giant Planets

In **Figure 1**, we plot the known densities of the regular satellites as a function of their distance from their primary in units of their respective primary's Hill radius $R_H = a(M_P/3M_\odot)^{1/3}$, for the three inner giant planets. The satellite sizes are scaled relative to each other. We label the centrifugal radius $r_c \approx R_H/48$, where R_H is the Hill radius of the primary, with a bold dashed line.

In this paper we pay special attention to comparing the properties of the satellites located inside $\sim R_H/100$. Inside Titan, Saturn's satellite system looks remarkably like that of Uranus, with the size (and perhaps the density) of the satellites correlating to the distance from the planet. The main difference being that the small Saturnian satellites (with the possible exception of Dione) appears to be made mostly of ice while those of Uranus are rocky (with the possible exception of Miranda). Interestingly, Jupiter's satellites become denser the

closer they are to the planet, whereas the opposite appears to be the case for those of Saturn (with the exception of Iapetus) and Uranus (though in the case of Uranus the evidence is less pronounced). If we compare the densities at $\sim R_H/100$ we find that Io is nearly ice free, Rhea is mostly ice, and Oberon is rocky.

We will argue that inside the centrifugal radius our model for the formation of the large, regular satellites does provide for a systematic view in which Saturn's satellite system bridges the gap between those of Jupiter and Uranus by combining the formation of a Galilean-type satellite (Titan), and the formation of smaller regular satellites, closer to the planet. Outside the centrifugal radius, there is again a sequence that leads to a smaller, farther out satellite for Saturn than for Jupiter. Since in our model a satellite the size of Iapetus is about the smallest size that can be left stranded, the absence of a regular satellite outside the centrifugal radius in the case of Uranus also follows from this sequence. We provide data on the known densities of the regular satellites of all three giant planets under consideration in **Table I**.

3 Satellite Evolution Due to Gas Drag and Tidal Torque

An object orbiting at Keplerian speed v_K will encounter a head-wind and drag towards the primary because the orbital velocity of the gas v_{gas} with density ρ_g is lowered by partial pressure support. A measure of the difference between the Keplerian velocity and the drag velocity is given by

$$\eta = \frac{v_K - v_{gas}}{v_K} \approx -\frac{r}{2\rho_g v_K^2}\frac{\partial P}{\partial r} \sim \left(\frac{c}{v_K}\right)^2, \qquad (1)$$

where P is the gas pressure, and c is the speed of sound. The timescale for evolution due to gas drag is given by

$$\tau_{gas} = \frac{4\rho_s r_p v_K}{3C_D(\Delta v)^2}\frac{2c}{\Omega\Sigma} \qquad (2)$$

where ρ_s and r_p are the satellitesimal density and radius, $C_D = 0.44$ is the Stokes flow regime drag coefficient for high Reynolds number, Ω is the orbital frequency, Σ is the gas surface density, and $\Delta v = \eta v_K$ (*e.g.* Weidenschilling 1988). Gas drag is most effective for smaller satellitesimals. However, for larger objects ($\gtrsim$ 1000 km), satellite migration is dominated by the tidal torque (see Paper I). In general, the tidal torque leads to migration because of the relative spacing of resonances inwards compared to outwards leads to a net torque that causes a satellitesimal to migrate towards the primary. The torque deposited at an mth order Lindblad resonance is given by (Ward 1997)

$$T_m = \epsilon\frac{4}{3}\mu^2(\Sigma a^2)(a\Omega)^2\frac{m^2\alpha_r^{3/2}\psi^2}{q\sqrt{1+\zeta^2}(1+4\zeta^2)} \qquad (3)$$

where μ is the ratio of satellite to primary mass, a is the satellite distance from the primary, m is the order of the Lindblad resonance, $\zeta \equiv mc/r\Omega$, and $\alpha_r \equiv r_L/a$ is the ratio of resonance location to satellite position. Here q is a weak function of ζ given by

$$q = 1 - \epsilon(1-l)h/\alpha_r^{3/2}\,\zeta/\sqrt{1+\zeta^2}, \qquad (4)$$

where $h = H/r$ is the normalized scale height. The factor $\epsilon = \pm 1$ depending on whether it is an inner or outer Lindblad resonance. The function ψ is given by

$$\psi = \frac{\pi}{2}\left[\frac{\alpha_r}{m}\left|\frac{db^m_{1/2}(\alpha_r)}{d\alpha_r}\right| + 2\sqrt{1+\zeta^2}b^m_{1/2}(\alpha_r)\right], \qquad (5)$$

(note that Eq. 5 corrects a typo in Ward (1997) where a factor of α_r was omitted) where the $b^m_{1/2}$ are the Laplace coefficients defined by

$$b^m_{1/2}(\alpha_r) \equiv \frac{2}{\pi}\int_0^\pi \frac{\cos m\phi\, d\phi}{\sqrt{1-2\alpha_r\cos\phi+\alpha_r^2}} \qquad (6)$$

The resonance location for a Lindblad resonance of order m is found by solving the condition for the frequency separation

$$D_* = \kappa^2 - m^2(\Omega-\Omega_s)^2 + (\Omega\zeta)^2 = 0 \qquad (7)$$

where κ is the local epicyclic frequency of the disk, $m\,|\Omega - \Omega_s|$ is the Doppler shifted forcing frequency, and Ω is the orbital frequency of the disk and is given by

$$\Omega^2 = \frac{GM_P}{r^3} - (k+l)\frac{c^2}{r^2} \qquad (8)$$

where $k \equiv -d\ln\Sigma/d\ln r$, and $l \equiv -d\ln T/d\ln r$ are the normalized density and temperature gradients, respectively. The first term is just the Keplerian rate, and the second term corrects for the radial support of the pressure gradient. The resonance condition can be written as

$$1 - \frac{\Omega_s}{\Omega} + \frac{\epsilon}{m}\left(\frac{\kappa}{\Omega}\right)\sqrt{1+\zeta^2} = 0 \qquad (9)$$

where we set $\kappa \approx \Omega$. Iterations are performed in order to find the resonant locations $r_L(m)$ for inner ($\epsilon = -1$) and outer ($\epsilon = 1$) Lindblad resonances for our model choices for k and l. For the inner disk we have $k = 1$ and $l = 1$. In the outer disk $k = 1$ and $l = 0 - 0.5$. In the transition region k can be as large as ~ 10. In **Figure 2** (see also Paper I) we specify the surface density and temperature of the subnebulae of Jupiter and Saturn at the time of satellite accretion. Care was exercised

to specify k so as to avoid having multiple resonance locations for one resonance wavenumber m.

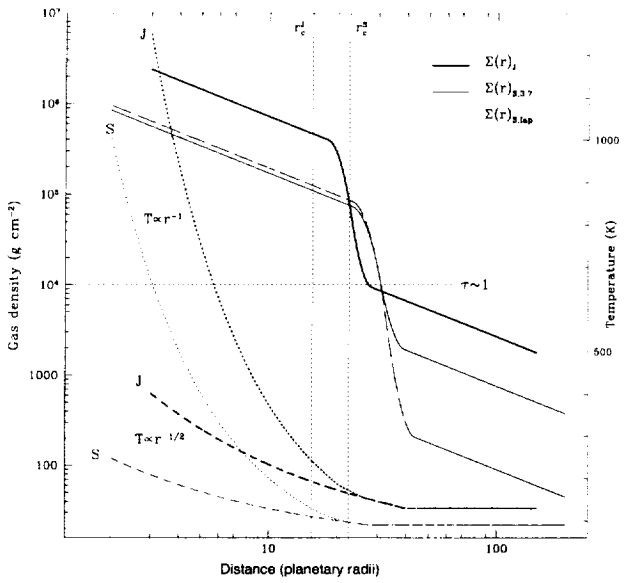

Figure 2: Gas surface density and mean photospheric temperature profiles for both Jupiter and Saturn used in this study. Bold lines refer to Jupiter. Optical depth unity ($\Sigma \sim 10^4$ g cm^{-2}) is labeled as well as the centrifugal radii of each body. Temperatures in the inner disk behave like r^{-1} while those in the immediate outer disk like $\sim r^{-1/2}$. The temperatures in the outer disk are taken to be that of the equilibrium solar nebula temperature ($T_e \approx 280\sqrt{1AU/r}$) which is roughly 130 K for Jupiter and 90 K for Saturn. The Jovian disk extends to $\sim 150R_J$ while both Saturnian models ("3.7" dotted line, "Iapetus" dashed line) extend to $\sim 200R_S$.

To calculate the torque we sum over resonances out to a value of $m >> a\Omega/c$, assuring that most of the torque has been included in the calculation. As pointed out by Ward (1997) such a torque produces mostly inwardly migrating satellites. The main reason for this is that the resonances outside the satellite occur closer to it than the corresponding resonances inside the satellite, resulting in a net torque that causes the satellite to drift inwards. A negative density gradient tends to decrease the net torque, whereas a negative temperature gradient increases it.

3.1 Survival of Callisto

Paper I deals with Callisto's slow formation, but it postpones discussion of Callisto's location. Now we turn to that issue. Though embryos grow as they drift, we consider it unlikely that embryos grew to a size such that they became stranded at Callisto's radial location. Had nothing acted to stall them or capture them, we expect that all the embryos forming in the outer disk would have drifted into the inner disk. Here we look for a mechanism to explain Callisto's radial location.

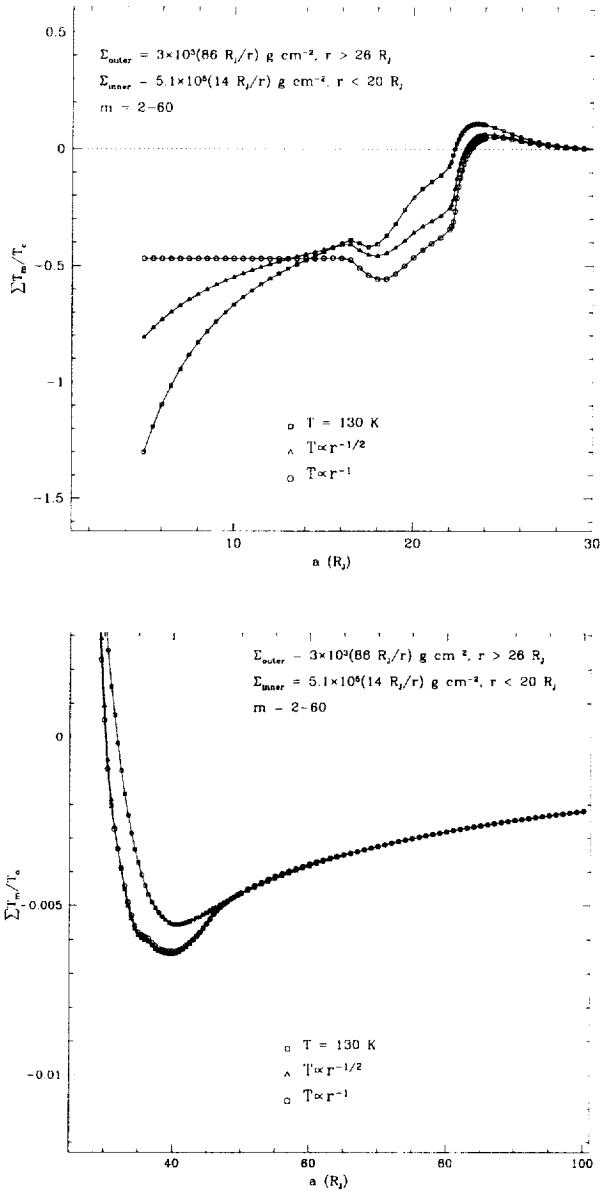

Figure 3: (a) Torque calculations for Jupiter's inner disk using various choices of the temperature profile (*cf.* Figure 2). Torques are scaled to the value of $T_c = 2.4 \times 10^{34}$ g cm^2 s^{-2}. (b) Torque calculations for Jupiter's outer disk.

As has been mentioned before, Ward (1997) pointed out that even in the presence of global density and temperature gradients tidal torques will in general lead to inward migration of large orbiting bodies. However, that study did not deal with the effects of local density gradients of the kind we envision here (see Figure 2), which occur over $\sim 2H_c$, where H_c is the scale-height at the centrifugal radius (and remain Rayleigh stable [e.g. Lin and Papaloizou 1993]). We now compute the

torque on a satellite placed in the inner and the outer subnebula gas disks. We normalize the torque to a reference value $T_c = \pi\mu^2\Sigma_c r_c^2 (r_c\Omega_c)^2/h_c^3$ where all quantities are evaluated at the centrifugal radius. To compute the torque we need to characterize the temperature as well as the density (see Figure 2 and Paper I).

In **Figure 3**, we show the torque exerted on the satellite as a function of radial distance for an outer disk gas density of $10^2 - 10^4$ g cm^{-2}, and inner disk gas densities of $10^4 - 10^6$ g cm^{-2}, for the two Jovian temperature profiles plotted in Figure 2 and a third constant temperature model. Here we have summed the torques for resonance numbers $m = 2 - 60$. Figure 3a corresponds to the torques in the inner disk. It can be seen that in a region between $\sim 20R_J$ and $30R_J$ the torques are actually positive, indicating that a proto-satellite placed there would exhibit outward migration no matter the specifics of the temperature profile (though the constant temperature peak is higher than the other two). Inside of $\sim 20R_J$, the torque again leads to inward migration.

The behavior of the different temperature profiles merits discussion. For a given scale height, a gradient in the temperature increases the magnitude of the migration inward (Ward 1997). It might seem puzzling, then, that as we approach the planet the constant 130 K temperature profile becomes more negative than the other two profiles. This is due to the torque-cutoff for resonances with $m > r/H$ (Goldreich and Tremaine 1980; Artymowicz 1993). The constant 130 K profile leads to a smaller scale-height than the other two profiles, which increases the number of resonances contributing to the total torque. As we approach the planet, the scale height of the constant temperature profile decreases rapidly, which leads to even larger torque magnitudes. By contrast, the curve with inner disk temperature profile $T \propto r^{-1}$ has constant r/H close to the planet. Thus, once the resonances no longer sample the transition region the torque becomes nearly constant as well.

In Figure 3b, we plot the torques in the outer disk. A net torque of zero is obtained near the location of Callisto, with the constant temperature profile occurring slightly further out. Since torques due to the gas dominate for large objects over migration due to gas drag, one would expect a proto-satellite to stall as it approached this location from either direction. As we move further out, all three profiles yield the same temperature and the torques merge.

In **Figure 4**, we decrease the amount of gas present in the inner disk by an order of magnitude and recompute the torques. In this case, though greatly reduced around $25R_J$, the torque never becomes positive anywhere in the disk. However, as we will see in section 4.1, a sharp drop in the tidal torque may be enough to explain the location of Callisto. It is worth noting that the constant temperature model again shows a more pronounced peak.

A region of positive torque certainly would help to account for the observation that the region between Callisto and Ganymede is empty, as well as help explain Callisto's large reservoir of angular momentum. If a satellite embryo $\sim$ 1000 km formed in the region of positive torque it might have evolved outward. Hence, it is possible that part of Callisto was derived from condensables drawn from the transition region (see Paper I); however, most of Callisto must be formed from materials in the outer disk if it is going to remain partially differentiated.

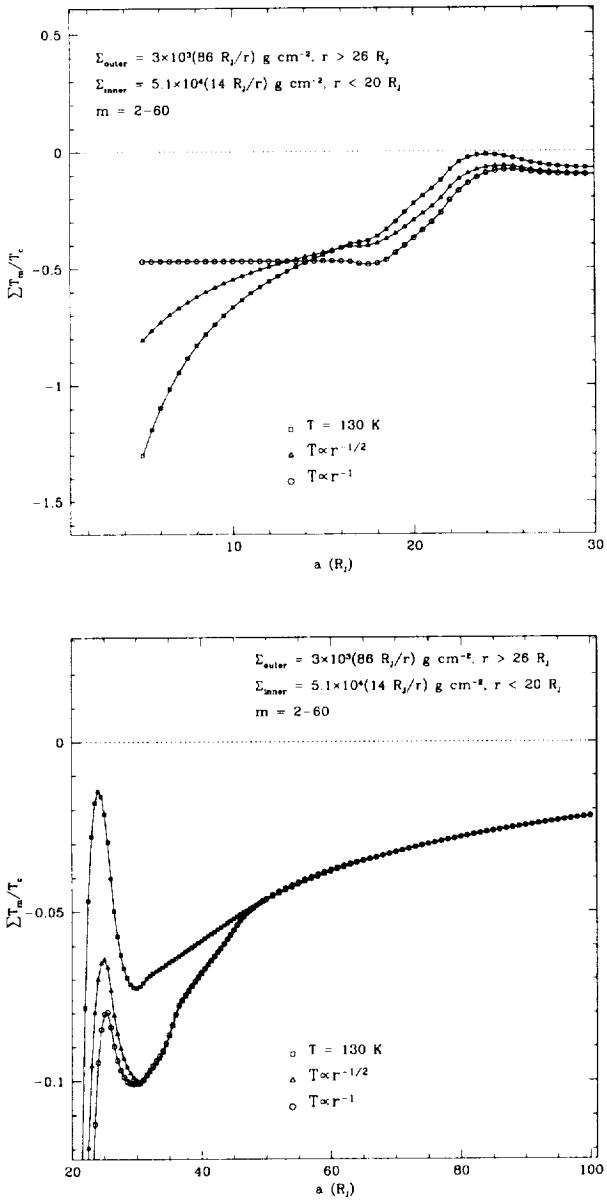

Figure 4: (a) Torque calculations for Jupiter's inner disk using various choices of the temperature profile (*cf.* Figure 2) for a gas surface density in the inner disk a factor of 10 less than in Figure 3. Torques are scaled to the value of $T_c = 2.4 \times 10^{33}$ g cm^2 s^{-2}. (b) Torque calculations for Jupiter's outer disk.

As we will see, our model for Saturn also turns out to have locations with zero torque which may not only account for the

presence of Iapetus, but may also explain why this satellite is so much further out in relation to Saturn than Callisto is from Jupiter.

None of this addresses the long term survival of satellites inside the centrifugal radius of giant planets. We tackle that issue in the next section.

4 Satellite Gap Opening

Given the ratio of the mass of the Galilean satellites to Jupiter it is natural to consider whether satellites can open a gap in the subnebula. Gap opening removes gas drag and ties the evolution of the satellite to the evolution of the disk. Consequently, it is worth exploring under what conditions one might expect satellites to open a gap.

Assuming local damping of the pressure waves, the criterion for a satellite of mass M_s to open a gap in the subnebula is (Goldreich and Tremaine 1980)

$$\mu = \frac{M_s}{M_p} > \left(\frac{c}{r\Omega}\right)_s^2 \alpha^{1/2} \tag{10}$$

where the gas viscosity is $\nu = \alpha c^2/\Omega$, and M_p is the mass of the planet. Using a lengthscale of the centrifugal radius $R_0 \sim r_c \sim 15R_J$, $T \sim 250$ K, and a timescale of $t_0 \sim 1000$ years (similar to Jupiter's gap-opening timescale) we get $\nu = R_0^2/t_0 \sim 10^{11} - 10^{12}$ cm^2 s^{-1}. This gives $\alpha \sim 10^{-4} - 10^{-3}$ and $M_s/M_p \sim 10^{-4}$, which gives $M_s \sim 10^{26}$ g. But one must remember that for our turbulence model the strength of the turbulence is variable both in space and in time. The end of planetary accretion will lead to weaker turbulence. Furthermore, in the outer region of the inner disk where the disk temperature approaches the subnebula temperature, the turbulence should be even weaker. Closer to the planet some remnant turbulence will continue until the disk becomes optically thin and/or the planet cools and the temperature approaches the background temperature. Since we expect Ganymede and Titan to have formed at a low temperature of 250 K and 100 K respectively, this would imply that the subnebula was only weakly turbulent at their position ($\alpha \sim 10^{-6}$; see Paper I). Therefore, both of these satellites are likely to have satisfied the above gap opening condition.

Lin and Papaloizou (1993) cite another condition that must be satisfied for the secondary to open a gap in the nebula; namely, the thermal condition $\mu \gtrsim h^3$, where $h = H/r$. As they point out, if the Roche lobe of the perturber is smaller than the scale-height of the subnebula, the gradient needed to produce a gap will be too steep and the gas will become Rayleigh unstable. This condition can also be seen as the criterion for non-linear dissipation of pressure waves to truncate the disk (Ward 1997). Although even Ganymede and Titan are too small to satisfy this condition, the fact that a perturber can open a gap several times its Roche-lobe probably means that the above criterion should be viewed as a loose indication of the size an object must be to make gap opening possible. Moreover, although the above may also be seen as the criterion for radial non-linear dissipation to allow for gap opening, three dimensional effects may allow for wave dissipation in the neighborhood of the secondary (Lin *et al* 1990a,b). Still, significantly smaller objects would find it difficult to clear material close to them in the presence of even weak turbulence. Thus, only Ganymede and Titan (and perhaps Callisto) are likely to have opened a gap in the subnebula. It is possible that these two satellites grew fast enough to avoid significant migration and then opened a gap in the gas (see Paper I). Further evolution would have taken place on the viscous timescale. Since the viscosity of the gas is expected to be weak (and to decrease with time) at the location of these satellites, they might have avoided significant migration altogether. That is, the present location of these satellites, just inside the centrifugal radius of their primary, may reflect the position of the satellite embryos that led to their formation.

However, it must be stressed that the disk's feedback reaction may cause a sufficiently large satellite to stall even if it does not open a gap. We can obtain a simple estimate of the inertial mass (Hourigan and Ward 1984; Ward and Hourigan 1989) in the inviscid limit by comparing the timescale $\tau_{drift} \approx (M_P/M_s)M_P h^3 P_s/\Sigma r^2$, where P_s is the satellite's orbital period, for a satellite to drift across H to the timescale for the satellite to change the surface density within H, $\tau_{grad} \approx h^6 P_s (M_P/M_s)^2$. The inertial mass is then given by $\mu_i = M_i/M_P \sim \Sigma r^2 h^3/M_P < h^3$. Hence in the inviscid limit the inertial mass criterion can be significantly smaller than the thermal condition (Lin and Papaloizou 1993). It is instructive to calculate the mass that would be required for the drift time τ_{drift} to be similar to the gap-opening time $\tau_{gap} \approx h^5 P_s (M_P/M_s)^2$. We get $\mu_{gap} = \mu_i/h$, which for the subnebula is O(10) larger than the inertial mass. Thus, we can see that it may be possible for a satellite to stall even if it does not open a gap in the subnebula. In such a situation satellite inward migration will continue at a rate determined by the viscous evolution of the gas disk. However, for low optical depth, quiescent disks this timescale may be longer than the timescale ($\sim 10^7$ years) for photodissociation or for solar wind to dissipate the gas. Hence stalling may lead to long term satellite survival.

The above discussion assumes that the density waves which carry the angular momentum are damped locally (*i.e.* close to the resonance location where the wave is launched). We now check whether this a good assumption in the present situation. For spiral density waves such that the Toomre parameter $Q_T = c\Omega/\pi G\Sigma >> 1$ the wave damping length is given by (Goldreich and Tremaine 1980)

$$x_{vis} \approx a \left(\frac{c^3}{m^{1/2}\nu a \Omega^2}\right)^{2/3}, \tag{11}$$

For our nebula parameters we find quite generally that $x_{vis} >> H$. This says that the wave launched by the satellite will damp much further away than the region where most of the torque is being deposited. As a result, this mechanism cannot be relied

upon to either open gaps in the subnebula or lead to satellite stall.

For sufficiently strong perturbations, non-linear damping of density waves will reduce the lengthscale from the value given above. In the low viscosity limit, the waves will damp when the perturbation of density in the wave approaches the density of the disk. At that distance shock dissipation would lead to effective wave dissipation and angular momentum deposition (Lubow and Shu 1975). For pressure waves the non-linear damping length is given by

$$x_{NL}^{P} \sim \frac{r^3 |\mathcal{D}| c^6}{\pi^2 \Psi_m^4}, \tag{12}$$

where $\Psi_m \sim (2m-1)GM_s/r$ is the forcing function of the secondary, and $|\mathcal{D}| \sim 3(m-1)\Omega^2$ (*e.g.* Ward 1986) with all quantities evaluated at the resonance location. This distance also turns out to be much larger than H. The waves travel a long distance before becoming non-linear, so this mechanism is not helpful in this context.

Here we simply adopt the damping model of Lin and Papaloizou (1993), who point out that for sufficiently large m the wavelength of inward traveling waves quickly becomes comparable to the scale height of the nebula. In a thermally stratified gas disk strong refraction turns the direction of propagation towards the disk surfaces. As the wave encounters low density regions far from the midplane non-linear damping can take place. It might be argued that this mechanism does not help in the context of satellites because wave refraction is weak in situations of low optical depth, whereas the timescale of orbital decay of a satellite in the presence of an optically thin gas disk is still short. While significant, we argue that this objection is not insurmountable for several reasons. We have already mentioned the possibility that micron-sized dust will keep the gas disk optically thick (see also Paper I). If so, wave refraction may take place as result. If not, gas turbulence as well as wave refraction will die down as the gas disk reaches an optical depth of order unity. This is significant because for a sufficiently quiescent disk the timescale for viscosity to even out gradients in the surface density of the gas may be comparable to the timescale for gas dissipation due to photodissociation or solar wind. In such a regime, weak wave refraction may suffice to preserve the surface density profile that led to a disk feedback reaction that caused the satellite's inward migration to stall in the first place. Furthermore, according to Tanaka and Ward (2000) inward traveling waves in an isothermal disk would also damp because the velocity of the perturbation becomes dependent on the vertical coordinate due to the changes in scale-height, and becomes so large at the disk surfaces that a shock wave would be formed (although we consider the isothermal case this is taken as an approximation of the cool planet limit; in actuality, we expect a weak temperature gradient will persist throughout the accretion of the regular satellites of the giant planets). Finally, non-linear damping at the disk surfaces may take place for reasons other than those mentioned above. For instance, for small satellites it may be invalid to assume (as has been done so far) that the location of the resonance is independent of the vertical coordinate. Relaxing this assumption may lead to vertical propagation of waves with wavenumber $m > r/H$. Given the theoretical uncertainty raised by these issues, we simply choose the damping length $x_{damp} = r_L/m$, where r_L is the radial location of the resonance. Next we look at the consequences of such a wave damping model.

4.1 Satellite Migration and Survival

In this section we consider Ward's (1997) criterion for a perturber migrating in an inviscid gas disk to stall. We add the effects of gas drag and non-local dissipation of angular momentum to make it applicable to cases where drift due to drag is comparable to drift due to torque, and the damping length is comparable to H. The following derivation follows that of Ward (1997).

The evolution of the disk is given by (Lynden-Bell and Pringle 1974)

$$2\pi r\Sigma\left(\frac{\partial L}{\partial t} + v\frac{\partial L}{\partial r}\right) = -\frac{\partial g}{\partial r} + \frac{dT^*}{dr}, \tag{13}$$

where $L = r^2\Omega$ is the specific angular momentum of disk material, $g = -2\pi\Sigma\nu r^3\partial\Omega/\partial r$ is the viscous couple, $v(r)$ is the radial velocity of disk material, and dT^*/dr is the torque density due to the angular momentum deposited by density waves where they damp. The continuity equation is given by

$$\frac{\partial\Sigma}{\partial t} + \frac{1}{r}\frac{\partial}{\partial r}(r\Sigma v) = 0. \tag{14}$$

The drift velocity of the satellite is given by a combination of the integrated torque density, and the local drag term

$$v_s = \frac{2}{M_s a\Omega_s}\int -\left(\frac{dT}{dr}\right)dr - \frac{a}{\tau_{gas}}, \tag{15}$$

As in Ward (1997), we find a solution for a surface density in the form of a kinematic wave. For the inner disk, $h = H/r =$ constant. This leads to the equation

$$3\pi\nu r^2\Omega\frac{\partial\Sigma}{\partial r} + \pi r^2\Sigma\Omega\left(v + \frac{3\nu}{2r}\right) = \frac{dT^*}{dr}. \tag{16}$$

By making the substitutions $\hat{\Sigma} = \Sigma/\Sigma_0$, $\hat{v} = v/a\Omega_s$, $\hat{\nu} = \nu/a^2\Omega_s$, $\hat{t} = \Omega_s t$, and $x = (r-a)/H_s$, we can reduce this set of equations to

$$\frac{3\hat{\nu}}{h}\frac{\partial\hat{\Sigma}}{\partial x} + \hat{\Sigma}\left(\hat{v} + \frac{3\hat{\nu}}{2}\right) = \frac{\mu^2}{h^4}\hat{\Sigma}F^*(x,k,l), \tag{17}$$

$$\frac{\partial \hat{\Sigma}}{\partial \hat{t}} + \frac{1}{h}\frac{\partial}{\partial x}(\hat{\Sigma}\hat{v}) = 0, \tag{18}$$

$$\hat{v}_s = -\frac{2\mu\mu_g}{h^3}\int \hat{\Sigma}F(x,k,l)dx - \hat{v}_d, \tag{19}$$

where $\mu_g = \pi\Sigma a^2/M_P$. The normalized torque density is given by

$$F(x,k,l) = \frac{h^4(dT/dr)}{\pi a^3\Omega_s^2\mu^2\Sigma}. \tag{20}$$

with a similar expression for the normalized and shifted torque density F^*. The assumed form for the kinematic wave implies from the continuity equation that $\hat{\Sigma}(\hat{v} - \hat{v}_s) = constant$. As seen from the secondary, the flux of disk material $2\pi\Sigma r(v - v_s)$ when evaluated at far enough distances such that the velocity is unaffected one can determine from (16) that $\Sigma(v - v_s) \rightarrow -\Sigma_0(3\nu/2a + v_s)$. We can then replace $\hat{\Sigma}\hat{v}$ with $(\hat{\Sigma} - 1)\hat{v}_s - 3\hat{\nu}/2$ in (17) to give Ward's (1997) equation (24)

$$\frac{3\hat{\nu}}{h}\frac{\partial \hat{\Sigma}}{\partial x} + (\hat{\Sigma} - 1)\left(\hat{v}_s + \frac{3\hat{\nu}}{2}\right) = \frac{\mu^2}{h^4}\hat{\Sigma}F^*(x,k,l). \tag{21}$$

A lower bound may be determined on the satellitesimal mass that may open a gap by setting the viscosity $\hat{\nu} = 0$. This leads to the density perturbation

$$\hat{\Sigma} = \left(1 - \frac{\mu^2 F^*}{h^4 \hat{v}_s}\right)^{-1}, \tag{22}$$

which may be substituted into equation (19) to yield after integration

$$\hat{v}_s \approx -\hat{V}\left(\Gamma_1 + \frac{\mu^2}{\hat{v}_s h^4}\Gamma_2^* + ...\right) - \hat{v}_d, \tag{23}$$

where $\hat{V} = 2\mu\mu_g/h^3$. The first term in parenthesis is proportional to the net disk torque $\Gamma_1 = \sum \hat{T}_m$, which represents the direct driving term. The second or "feedback" term is proportional to Γ_2^* (defined by Equations [26] and [27]). It should be noted that since the drift velocity includes a drag contribution the "feedback" term does as well. We can solve to lowest order for the motion of the satellitesimal

$$\hat{v}_s = -\frac{\hat{V}}{2}(\Gamma_1 + \Gamma_d)(1 \pm \sqrt{1 - \mu/\mu_{i,d}}), \tag{24}$$

with $\Gamma_d \equiv \hat{v}_d/\hat{V}$. The modified inertial mass (Hourigan and Ward 1984; Ward and Hourigan 1989) taking into account the gas drag drift velocity is given by

$$\mu_{i,d} = \mu_g h\frac{(\Gamma_1 + \Gamma_d)^2}{2\Gamma_2^*}. \tag{25}$$

The quantity Γ_1 is obtained by adding inner and outer torques. The contribution due to angular momentum deposition at the location of damping Γ_2^* may be obtained from

$$\Gamma_2^* = H_s\sum \frac{m\hat{T}_m}{2\kappa}\left|\frac{dD_*}{dr}\right|\sum_{n\geq m}\hat{G}_n, \tag{26}$$

where

$$\hat{G}_n = \begin{cases} \hat{T}_n, & r_L^{m+1} < r_L^n + x_{damp} \leq r_L^m;\ \epsilon = 1 \\ \hat{T}_n, & r_L^m \leq r_L^n - x_{damp} < r_L^{m+1};\ \epsilon = -1 \\ 0, & \text{otherwise} \end{cases} \tag{27}$$

is a sum over torque contributions deposited at the distance $x_{damp} = r_L/m$ from the location r_L where the wave is launched.

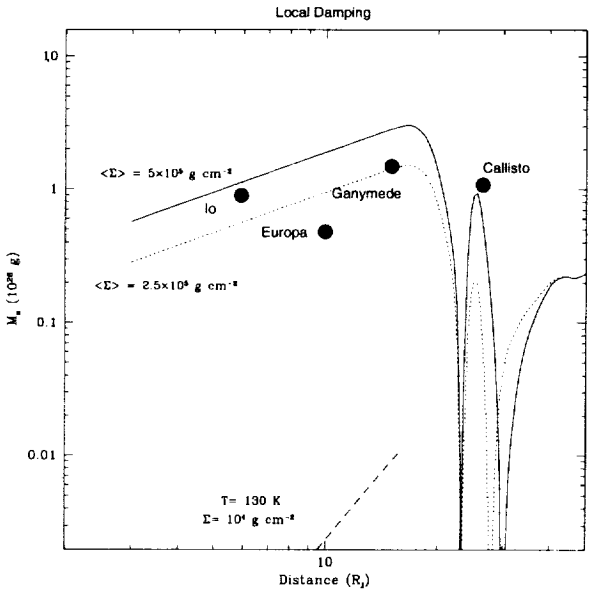

Figure 5a: Inviscid inertial mass for the Jovian system for $\rho_s = 2$ g cm^{-3} and for various gas surface density models using local damping of pressure waves. The solid line corresponds to our initial temperature and density profile for Jupiter. The dotted corresponds to a decrease of the mean surface density of the inner disk. The dashed line is a constant temperature and constant surface density model where $\Sigma = 10^4$ g cm^{-2} which corresponds to a gas optical depth of $\tau \sim 1$.

In **Figure 5**, we plot the inertial mass as a function of distance from the planet for a sequence of disk models with

decreasing gas surface density for the inner disk assuming $\rho_s = 2.0$ g cm^{-3}. The solid curve corresponds to our initial model for the density and temperature of Jupiter's disk as plotted in Figure 2 (which has an average surface density of 5×10^5 g cm^{-2}). The dotted curve corresponds to a later time such that the turbulence in the inner disk has lowered the gas surface density there to the average value given in the plot. The radial dependence of the surface density is assumed to remain $\propto r^{-1}$, and the outer disk gas density is left unchanged since the gas is expected to be quiescent there. The dashed curve corresponds to a later time in which the gas is taken to be of optical depth order unity with $\Sigma \sim 10^4$ g cm^{-2} everywhere in the inner disk and the subnebula temperature is the solar nebula temperature at Jupiter's location. We picked a cool disk with surface density of 10^4 g cm^{-2} for comparison with Saturn (whose satellite system accretion time is longer and cools much faster), and also because the subnebula turbulence is likely to die down as the disk becomes optically thin. It also bears pointing out that the criterion for the inertial mass was obtained in the inviscid limit, whereas turbulence is used to remove gas from the inner disk. Here again we stress that the post-accretion turbulence is taken to be quite weak (it must be weak to avoid heating up the gas disk and preventing water condensation [see Paper I]) and may die down even further on the satellite accretion timescale, so that the inviscid approximation may apply.

Figure 5a corresponds to the case where the damping is assumed to be local. In that case the turbulence needs to lower the gas density by about a factor of 2 for the inward migration of Ganymede and Io to stall. Europa appears to be too small to stall even then, but this conclusion may be complicated by its proximity to a resonance with Io. Given our nominal post-accretion turbulence parameter in the range $\alpha \sim 10^{-5} - 10^{-6}$, the timescale for the disk to evolve is $10^4 - 10^5$ years (see Paper I), which is somewhat longer than the accretion timescale for the Galilean satellites. This suggests that it may be reasonable to consider a disk with solid concentration larger than solar. Even a moderate increase in concentration would have a significant effect since it would lower the amount of gas that needs to be removed for the satellites to stall, and it would also allow for stronger turbulence for a given temperature profile. In this figure it can also be seen that Callisto would stall for all the curves. The reason for this is that Callisto's torque and drift velocity is much smaller in magnitude (given its location in the plot, in the absence of a disk feedback reaction, its drift would be outward) than for the inner satellites. Clearly present in this figure are the two locations of zero torque, which correspond to locations where a satellite will stall regardless of its size (provided there is no gas drag). Notice that Callisto stalls even when the surface density of the inner disk has dropped by about an order of magnitude. This corresponds to a case in which the torque becomes small but never zero (see Figure 4). In this case, the inertial mass curve develops a single dip around the location of Callisto. It is clear, then, that the torque of the disk at Callisto's location need not be exactly equal to zero for this satellite to stall. Any significant drop in the value of the net tidal torque will make it more likely that Callisto will stall outside the centrifugal radius, near its present location.

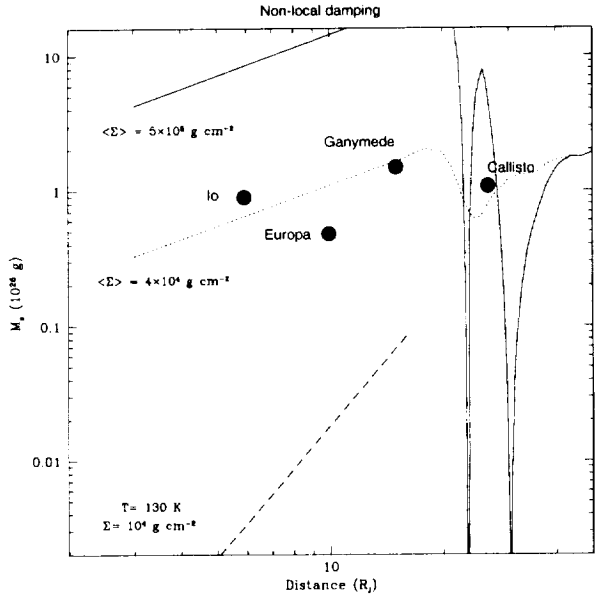

Figure 5b: Inviscid inertial mass calculations for the Jovian system for $\rho_s = 2$ g cm^{-3} and for various gas surface density models using non-local damping. Note that $\Sigma = 10^4$ g cm^{-2} corresponds to a gas optical depth of $\tau \sim 1$.

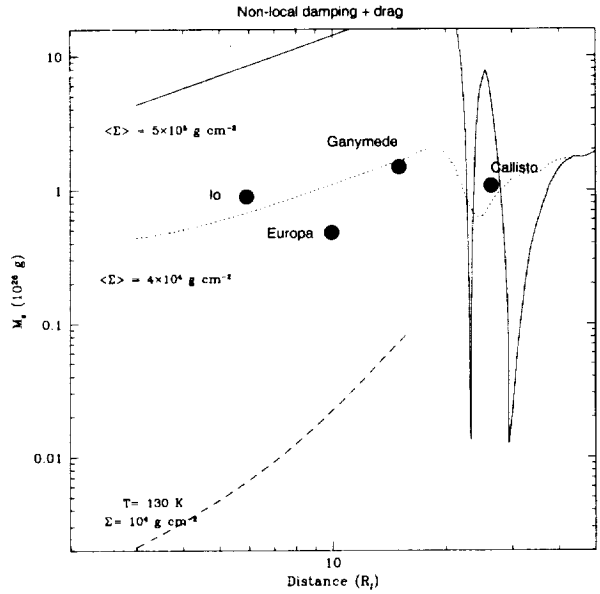

Figure 5c: Inviscid inertial mass calculations for the Jovian system for $\rho_s = 2$ g cm^{-3} and for various gas surface density models using non-local damping and effects due to gas drag. Note that $\Sigma = 10^4$ g cm^{-2} corresponds to a gas optical depth of $\tau \sim 1$.

Figure 5b corresponds to the case where the damping is done non-locally. As expected, non-local effects make it more difficult for a satellite to stall. In this case the gas turbulence

would have to remove about an order of magnitude of gas before the satellites can stall (with Europa significantly below the curve). As before, the location of zero torque leads to zero inertial masses, since any satellite that drifts into this location will experience no net torque and will stall. Finally, we add drag and obtain Figure 5c. The only noticeable difference between Figure 5b and 5c is the shape of the curves in the low mass region of the plot (but note that in this case a satellite drifts even placed at the location of zero torque). A constant temperature and constant surface density disk (dashed curve) might seem to imply no gas drag, but at the midplane the pressure gradient would still be non-zero (due to the gradient in volume density) so drag is present for that curve as well.

From these figures one can see that in general the inertial mass (or mass that will stall in the inviscid limit) increases with distance. The reason for this is that the non-dimensional disk mass μ_g decreases closer to the planet despite the increase of surface density. In fact for $\Sigma \propto r^{-1}$ it is easy to see that $\mu_g \propto r$. This allows a satellite to drift until it finds an equilibrium position, so long as it is sufficiently massive to stall somewhere in the disk. Nevertheless, in the presence of a strong temperature gradient the slope is shallow, and the range of masses that can satisfy the condition for stalling is narrow. Still, one can see that it is possible for Ganymede to find an equilibrium location far out in the disk while Io finds it closer in. From the dashed curve we see that for the case of an isothermal, constant surface density gas disk the slope is much steeper; thus, presumably allowing much smaller satellites to stall closer in to the planet. The reason for this is related to the torque cut-off phenomenon. A constant temperature disk leads to relatively smaller scale-heights as we approach the planet. A smaller scale-height means that more resonances provide a contribution to the torque. As a result, the feedback reaction of the torque increases and even a relatively small mass object can satisfy the condition for stall. Since its cooling time is comparable to the gas dissipation timescale $\sim 10^7$ years, Jupiter may not have cooled fast enough to allow for an isothermal disk. We will see later on that Saturn may have.

It must be stressed that the inertial mass criterion is not equivalent to one in which one compares the gap opening timescale to the drift timescale. Even if a satellite is assumed to open a gap, it would do so on a timescale considerably longer than the time it takes for the satellite to drift a distance equal to the gap size. Even so, the inertial mass criterion still predicts that the satellites would stall. The reason for this is that stalling does not require a gap to form, only that the surface density in the neighborhood of the satellite be sufficiently altered by the satellite's presence to effectively oppose its migration.

5 Saturn's Satellite System

In this section we perform analogous calculations for Saturn with subnebula surface density and temperature as given in Figure 2. There it can be seen that a "minimum mass" model gives a generally lower surface density for Saturn. Also as expected the initial temperature profile is generally cooler. It is particularly interesting to ask how long after the end of planetary accretion do regions inside of $r \sim R_H/100$ (this corresponds to the location of Io for Jupiter and Rhea for Saturn; see Figure 1) become sufficiently cool for water condensation. For low opacity disks Pollack *et al.* (1976) give a time of $10^5 - 10^6$ years for Saturn and $\sim 10^7$ years for Jupiter for this location to cool to ~ 250 K, where we compare low opacity cases because the cooling timescale is sufficiently long for even weak turbulence to remove most of the gas in the subnebula. Given that Io is nearly ice-free yet Rhea is icy, it should be clear that this is potentially a very important distinction between Jupiter and Saturn. We will discuss this issue in detail in sections 5.2 and 5.3. Now we turn to Saturn's outer disk.

5.1 Survival of Iapetus

A possible explanation for the location of Iapetus at $\sim 60R_S$ is that this was the position of zero torque of the subnebula before the time of gas dissipation. In **Figure 6**, we plot the torques as a function of position for the inner and outer disks, and for the two gas density models of Figure 2. Each panel displays curves that correspond to the Saturnian temperature profiles of Figure 2, plus a constant temperature profile corresponding to the solar nebula temperature at Saturn. These plots have much the same features as those for Jupiter, except that the region of positive torque has broadened considerably. The outer location of zero torque is now found at $\sim 45R_S$ for the 3.7 model, and at $\sim 60R_S$ for the Iapetus model (i.e. a model in which just enough mass is placed outside Iapetus' orbit to form this satellite). These locations are considerably farther out than was the case for Jupiter. Though the exact location of zero torque is (weakly) dependent on the width of the transition region (a more extended transition region leads to a zero torque location slightly closer to the planet), we find that for Saturn this location occurs further out than in Jupiter mostly because of Saturn's larger Hill radius and less massive outer disk. Hence the position of zero torque may help to explain how a non-captured object may be left stranded at such a large radius. Given our subnebula parameters the transition from a gas drag dominated regime to a tidal torque dominated regime takes place between particles of size 500 to 1000 km (gas drag is larger for the former particle and weaker for the latter; see Figure 5b, Paper I). Thus, Iapetus may be regarded as a loose cut-off size below which one would not expect the subnebula tidal torque to be able to strand particles outside the centrifugal radius. It is also possible, however, that there wasn't sufficient drag or tidal torque for this object to drag further in a timescale less than 10^7 years and it was left stranded.

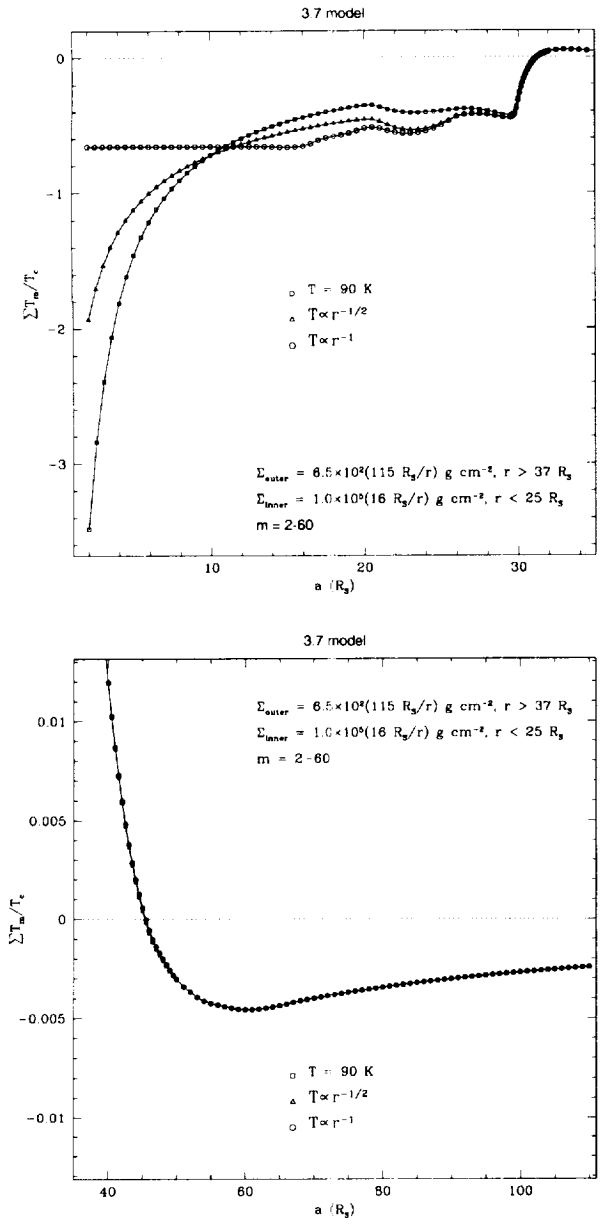

Figure 6: (a) Torque calculations for Saturn's inner disk using various choices of the temperature profile (*cf.* Figure 2) for the "3.7" model. Torques are scaled to the value of $T_c = 7.6 \times 10^{33}$ g cm^2 s^{-2}. (b) Torque calculations for Saturn's outer disk using the "3.7" model.

5.2 Satellites inside of Titan

As we noted in Paper I, there are several important features that characterize the satellites that are found inside the orbit of Titan. With the possible exception of Dione, they all have densities consistent with icy bodies (see Table I). They are all small compared to Titan (adding up to only $\sim$ 3 % of the total mass of the satellite system). They are found well inside the centrifugal radius of the primary (see Figure 1); and perhaps most importantly, they are ordered by size, with the larger satellites further out. There are two mechanisms that can lead to such a distribution of sizes. One is outward tidal expansion of the satellite orbits. However, it can be shown that to significantly alter the position of Rhea over the lifetime of the solar system would require Saturn's tidal dissipation parameter to be smaller than the lower bound set by the present position of Mimas at $3.1R_S$, even if it started as far in as the co-rotation radius at $1.8R_S$. Moreover, the absence of Mimas size satellites far from the planet cannot be explained by tidal effects. Therefore, size sorting cannot be the result of tidal effects alone (though tidal forces may explain the Tethys-Mimas and Dione-Enceladus resonances, as well as the evidence for endogenic activity in Enceladus and Tethys). The other option is to explain size sorting by gas drag and/or tidal torque. We have already argued that Titan may have formed fast enough to avoid significant migration either due to gas drag or gas torque before opening a gap in the subnebula. On the other hand, the inner satellites are probably much too small to have opened gaps even in the presence of even weak turbulence. The puzzle then becomes the fact that they survived at all.

Interestingly, the orbital decay timescale (gas drag plus tidal torque) for midsize Saturnian satellites (200 – 700 km) is much longer ($10^4 - 10^5$ years) than the orbital decay timescale for Titan ($\sim$ 100 years!). This is a result of the much weaker tidal torque for the smaller objects (see also Paper I). Furthermore, close to the planet even weak turbulence ($\alpha \sim 10^{-5}$) may lead to viscous dissipation of the inner gas disk on a timescale comparable to the orbital timescale for these objects. This raises the possibility that turbulence is responsible for stranding these satellites. However, since the orbital decay time over this size range is not necessarily a monotonic function of satellite size, it is unclear that such a mechanism will produce the observed mass versus distance distribution of satellites. Moreover, we expect gas turbulence to die down once the gas disk approaches optical depth of order unity. Thus, one might need to rely upon hypervelocity impacts to kick up sufficient quantities of micron-sized dust to keep the inner gas disk optically thick. Nevertheless, we cannot rule out this possibility at this time.

We suggest that the inner satellites began to form at the tail end of Titan's accretion. We argue that the formation of these satellites took place $> 10^5$ years after Saturn's accretion, once the temperature had dropped enough to condense water inside of $\sim 8R_S$. Given our model, the size of this inner region where icy satellites were formed is determined by the location at which the temperature in the optically thick disk starts out > 250 K.

It might be argued that the planet begins to cool immediately, so that the above time delay is arbitrary, but it must be remembered that as the disk loses gas and becomes optically thin, its temperature at a given radius will increase if the viscous timescale is shorter than the planetary cooling timescale.

Since it takes $10^5 - 10^6$ years for an optically thin disk to reach a temperature of 250 K at $8R_S$ (Pollack *et al.* 1976) condensed water may have been unavailable inside of that radius for that long. This time may have been long enough that viscous evolution, even assuming weak turbulence, would have lowered the density of the gas disk to an optically thin value (at which time the turbulence may have died down, provided the dust opacity were also low). Once it became cool enough for water condensation, the inner disk would be water enriched due to the evaporation before that time of inwardly drifting particles from outside $8R_S$. Furthermore, most of the silicates in the disk not accreted by Titan may have been lost by then, hence the satellites ended up mostly made of water ice (but possibly ammonia and methane as well).

We now ask whether a disk with surface density of 10^4 g cm^{-2} has enough water in it to produce the inner satellites of Saturn. Not surprisingly a straightforward solar mixtures calculation yields too little mass out to $8R_S$ by about an order of magnitude. As we mentioned above, the inner portion of the disk may have been water enriched. However, a detailed calculation will be left for further work.

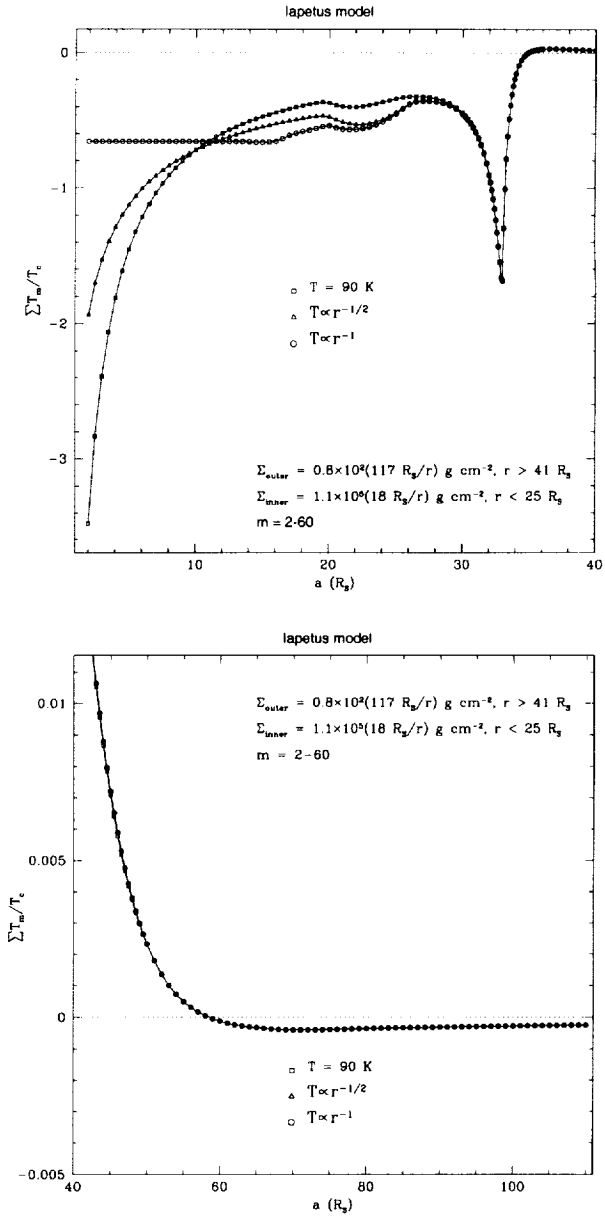

Figure 6: (c) Torque calculations for Saturn's inner disk using various choices of the temperature profile (*cf.* Figure 2) for the "Iapetus" model. Torques are scaled to the value of $T_c = 8.7 \times 10^{33}$ g cm^2 s^{-2}.(d) Torque calculations for Saturn's outer disk using the "Iapetus" model.

5.3 Saturnian Satellite Migration and Survival

A satellite may not need to open a gap to survive. Rather, the feedback reaction of the disk may stall its inward migration even before a gap forms, and allow the satellite to survive long enough for gas dissipation to take place. In section 4.1, we adapted the inviscid inertial mass criterion to a situation to include non-local damping and the effects of gas drag. For Jupiter we argued that the inviscid limit may not be bad, since by the time the satellites have completed their accretion the surface gas density of the disk was probably close to optical depth of order unity. For Saturn, too, the inviscid limit may be applicable: Saturn's turbulence may have been weaker than that of Jupiter (particularly at the location of Titan, where the temperature of the subnebula is close to the solar nebula temperature at Saturn's location).

Why, however, are there no large satellites $r_s > 1000$ km inside the orbit of Titan? We can think of five possible reasons for this. The first one involves a combination of Saturn's longer satellite accretion time combined with the early bombardment of planetesimals from the edge of the Roche-lobe. Bombardment may prevent satellite formation because close to the planet collisional events might have been energetic enough to disrupt satellite embryos (Greenberg *et al.* 1977).

However, Saturn's weaker turbulence (and more concentrated particle layer) may shorten its embryo formation timescale. Hence, though this explanation is plausible, it is not clear that Saturn's embryos would have been more vulnerable than those of Jupiter. The second reason is related to the possibility that, by removing gas from the disk and increasing the concentration of solids, some turbulence helps satellites to survive. Given the weaker temperature gradient and faster cooling of Saturn's disk, its turbulence may have been correspondingly weaker and more short-lived than that of Jupiter's disk. That is, even though Saturn started out with less gas, its weaker turbulence might have allowed gas to remain longer. It is possible, then, that the gas density in Saturn simply stayed too high for the large satellites that formed there to stall and survive. Furthermore, while by leading to a thin particle layer weaker turbulence may lead to faster embryo accretion times, it may actually delay the formation of a full size satellite (see Paper I). Which of these two explanations is correct depends on the relative strength of the turbulence of the subnebulae of the two planets as a function of time. Both explanations benefit from the smaller embryo sizes typical of Saturn's disk (see Paper I). Smaller embryos are more likely to breakup and/or fail to stall, and be lost to the planet. Unfortunately, our model indicates that initially at least the turbulence of the two planets was likely to be of the same order of magnitude (see Paper I). Hence it is difficult to decide in favor of one explanation over the other. A third possibility is that the concentration of solids was substantially greater in the subnebula of Jupiter than in the subnebula of Saturn (though the rough parity between the mass ratio of atmospheric envelopes and cumulative satellite masses argues against it). The fourth possibility is that by effectively scattering planetesimals as it accreted Jupiter may have reduced the bombardment of late arriving planetesimals, thus partially shielding its proto-satellite system. The fifth possibility is that Jupiter's stronger temperature gradient (both vertically and radially) leads to stronger damping of pressure waves and a stronger feedback reaction of the gas disk to the presence of the satellite, making it easier for satellites to stall. One might expect this to be the case if the vertical refraction of the pressure waves (Lin and Papaloizou 1993) leads to damping distances much smaller than the scale-height. Stronger wave damping may also explain why the Galilean satellites are further below the inertial mass curves than Titan for a given damping model (see Section 5.3).

At any rate, it is likely that Io and Europa formed inside Ganymede at a time when the temperature was too high for water condensation, thus these satellites ended up nearly ice-free. The reverse might be true for the satellites found inside of Titan. We have already seen how a constant temperature disk allows for relatively small objects (between 100 and 1000 km) to find a radius close to the planet where the feedback reaction of the disk allows their inward migration to stall. In the case of Jupiter no such objects are observed. This may be because Jupiter did not cool fast enough to allow for it. On the other hand, Saturn's shorter cooling time means that water condensation in the inner disk takes place before complete gas dissipation (here presumed to take place in 10^7 years), but probably after the gas turbulence resulted in a disk with optical depth order unity. Hence, we delay formation of the inner satellites to allow time for planetary cooling. By the time the inner satellites of Saturn (inside of $8R_S$) accreted (see Paper I), the disk around Saturn was likely to be nearly quiescent and cool.

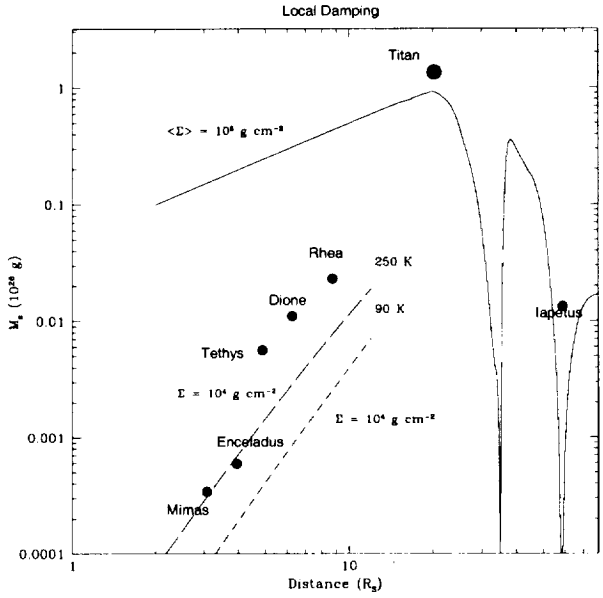

Figure 7a: Inviscid inertial mass calculations for the Saturnian system (Iapetus model) for $\rho_s = 1.5$ g cm^{-3} and for various gas surface density models using only local damping. The solid line corresponds to our initial temperature and density profile for Saturn. The dashed line is a constant temperature and constant surface density model where $\Sigma = 10^4$ g cm^{-2} which corresponds to a gas optical depth of $\tau \sim 1$. For the long dash line the temperature is 250 K. For the short dash line the temperature is 90 K.

In **Figure 7**, we plot the inviscid inertial mass as a function of distance for (a) local damping, (b) non-local damping, and (c) non-local damping and gas drag for $\rho_s = 1.5$ g cm^{-3}. The solid curves in each of these correspond to the optically thick model specified at the outset, with gas density and temperature profile as in Figure 2 (Iapetus model). The dotted curves still correspond to an optically thick model, except that the average surface density is now presumed to be lower due to the effects of gas turbulence. Finally, the dashed curves corresponds to a gas optical depth of order unity, with constant surface density and temperature. The long dash corresponds to the water condensation temperature 250 K and the short dash curve has a temperature equal to the background temperature $\sim$ 90 K.

As expected non-local damping makes it considerably more difficult for a satellite to stall. In the case of Titan, our non-local damping model requires that turbulence remove significant amounts of gas by the time the satellite completes its accretion in $10^4 - 10^5$ years, whereas the local damping model puts Titan well over the inertial mass that would lead to

satellite stall. Also as expected gas drag has no effect on this satellite. As was the case with Callisto, Iapetus finds it easy to stall due to the nearby location of zero torque even when gas drag is included (recall that in the presence of gas drag a satellite may continue to drift even at the location of zero net torque). These plots also show that given its location close to the outer position of zero torque, Iapetus is likely to stall regardless of the specifics of the model under consideration (but note that the size of Iapetus is close to the cut-off size such that the tidal torque dominates the gas drag). This offers an explanation for the present day location of Iapetus.

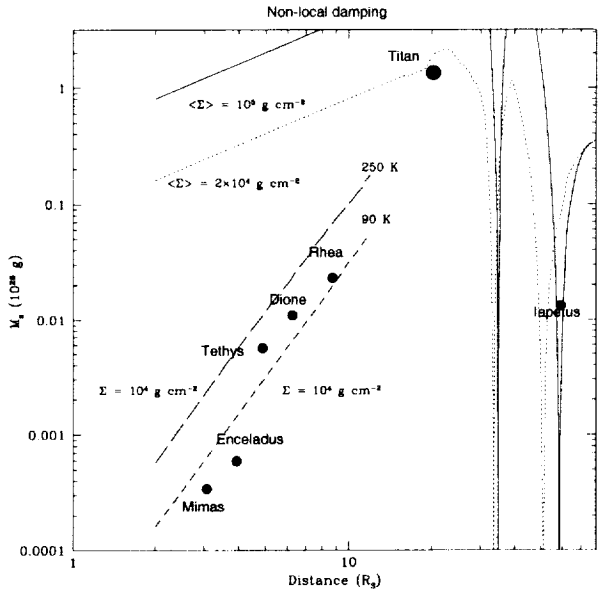

Figure 7b: Inviscid inertial mass calculations for the Saturnian system (Iapetus model) for $\rho_s = 1.5$ g cm^{-3} and for various gas surface density models using non-local damping. Note for the dashed lines, $\Sigma = 10^4$ g cm^{-2} which corresponds to a gas optical depth of $\tau \sim 1$.

Whereas the corresponding plots for Jupiter exhibited no satellites close to the background temperature curve, the inner Saturnian satellites now provide a very good fit to the bottom dashed curve in Figure 7b (which includes the effects of non-local damping), and Figure 7c (which includes both non-local damping and gas drag). Though the fit in Figure 7b is tantalizing, it is unlikely that the pressure gradient is sufficiently small that the effects of gas drag can be ignored. Furthermore, we expect the location of Mimas to be significantly altered by the effects of planetary tides. A constant surface density and constant temperature torque has gas drag because of the non-zero pressure gradient at the midplane (due to the gradient in volume density). Therefore, we consider the constant temperature fit of Figure 7c to be more satisfactory in that it matches the positions of the outermost and most massive inner satellites, for which our results are applicable. To produce this plot the masses of the inner satellites were corrected in order to take into account the effect of their variable density. The reason for this is that the actual gas drag a satellite experiences depends on its density as well as its size, while the model curve for Figure 7c was calculated using a density of 1.5 g cm^{-3}. The corrected mass for the inner satellites is given in **Table II**. These masses were obtained using

$$M_s^* = M_s \frac{(\Gamma_1 + \Gamma_d)^2}{(\Gamma_1 + (\rho_s/\rho_s^*)^{2/3}\Gamma_d)^2}, \tag{28}$$

where ρ_s^* is the actual density of the satellite, to be consistent with the surface density Σ and the satellitesimal density ρ_s of the model curves. Since the Galilean satellites are not affected by drag, their effective masses are very close to their actual mass.

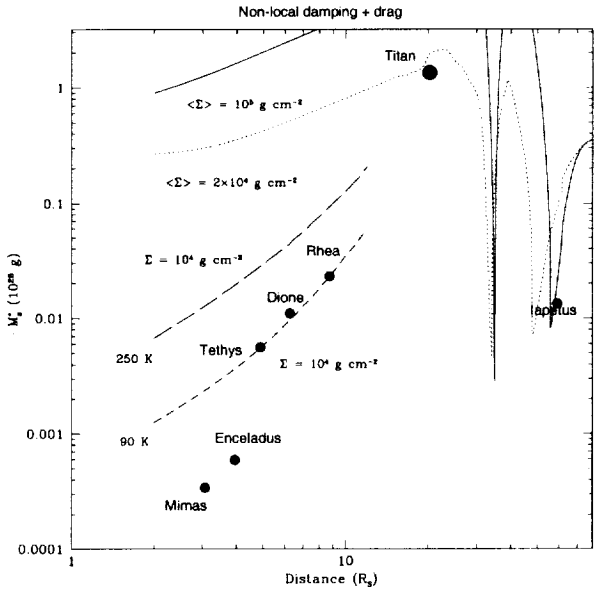

Figure 7c: Inertial mass calculations for the Saturnian system (Iapetus model) for $\rho_s = 1.5$ g cm^{-3} and for various gas surface density models using non-local damping and effects due to gas drag. Note for the dashed lines, $\Sigma = 10^4$ g cm^{-2} which corresponds to a gas optical depth of $\tau \sim 1$. The masses of Mimas, Enceladus, and Tethys have been corrected to take into account their actual densities.

In order to interpret the cool, constant density fit as being meaningful one has to consider whether this case can represent the final location of the satellites. Because the satellites inside Titan are icy, we expect that they formed at a temperature of $\sim$ 250 K. We can see from Figure 7 that for a given damping model the 250K curve lies above the 90 K curve (a hotter subnebula leads to a larger scale-height and a more pronounced torque cutoff). Since the satellite migration timescales are considerably faster than the planetary cooling timescales, this may seem to indicate that these satellites should have moved in further following their accretion, which would invalidate the background temperature fit to their current locations. However, one must keep in mind that the wave damping mecha-

nism we rely on is more effective in the presence of strong wave refraction (Lin and Papaloizou 1993). It is likely, then, that a hotter disk would lead to stronger wave refraction and shorter damping distances. In this regard, we point out that the 250 K long dash curve falls well below the satellites in the local-damping case (Figure 7a). Even though careful modeling will have to be performed to verify this possibility, we suggest that it is likely that these satellites continued migrating inwards, albeit slowly, as the planet cooled. If so, their present locations would correspond to the cool disk conditions at the tail end of their evolution.

TABLE II
Adjusted Satellite Masses M_s^*

Satellite	M_s (10^{26} g)	M_s^* (10^{26} g)
Saturn		
Mimas	3.7×10^{-4}	3.4×10^{-4}
Enceladus	6.5×10^{-4}	5.9×10^{-4}
Tethys	6.1×10^{-3}	5.6×10^{-3}
Dione	0.011	0.011
Rhea	0.023	0.023
Uranus		
Miranda	6.59×10^{-4}	6.3×10^{-4}
Ariel	0.0135	0.014
Umbriel	0.0117	0.0117
Titania	0.0353	0.0353
Oberon	0.0301	0.0301

It is important to note that for the inertial mass curve to be strictly meaningful the satellites must be separated by a distance that allows the waves to damp before they reach the nearest neighbor. To see if this is the case, we compare the separation between the inner Saturnian satellites to the sum of the distance between the maximum of Γ_2^* (the disk feedback term) for the inner torques of an outer satellite and the outer torques of its inner neighbor. The results are $2.7R_S$ for the Rhea-Dione pair compared to an actual separation of $2.5R_S$, and $1.6R_S$ for the Dione-Tethys pair compared to an actual separation of $1.4R_S$. It is also useful to write the separation of these moons in terms of the average scale-height at their location given a temperature of $90K$. In units of the average scale-height the separations are Mimas-Enceladus $3.8H_{ME}$, Enceladus-Tethys $2.9H_{ET}$, Tethys-Dione $3.0H_{TD}$, and Dione-Rhea $3.5H_{DR}$. Hence the positions of the Saturnian inner moons are consistent with our stalling mechanism.

It might be argued that such a mechanism can only produce a distance to mass relationship if the smaller moons form further out than the larger moons in the first place. However, this argument ignores the possibility that moons can "horseshoe" past each other as they seek an equilibrium location. While the possibility of this happening may be less than 0.5, it is certainly not negligible. Furthermore, two moons may coalesce while the disk is hot, and find a combined equilibrium location when the disk cools. Nevertheless, a strict mass to distance relationship is certainly not the only possible outcome. For one thing, collisional events taking place after gas dissipation may alter the positions of the moons. In general, we would expect that this mechanism would tend to produce a mass to distance correlation between moons with a significant amount of scatter. As we shall see, this interpretation may be consistent with the Uranian moons as well.

As shown by the corrected inviscid inertial mass criterion, then, a nearly constant temperature profile allows midsize satellites to stall and survive until gas dissipation. Furthermore, because they formed later, these satellites might have avoided heavy Roche-lobe bombardment (though evidence of bombardment is clearly present). Such satellites would be made mostly of water because only water was available to them when they formed $10^5 - 10^6$ years after Saturn's accretion.

6 Uranian Satellite System

Like the inner satellites of Saturn, the satellites of Uranus are all well inside the centrifugal radius of the primary (see Figure 1). There is also evidence here of size sorting and even of endogenic activity! The main difference with Saturn appears to be that these satellites are considerably denser than the inner Saturnian satellites. Only Miranda has density (1.2 g cm^{-3}) consistent with an icy body.

A "minimum mass" model (where the size of the disk is determined by the location of the centrifugal radius at $57R_U$) puts the gas density at $\sim 10^4$ g cm^{-2}. Therefore, we expect a cool, largely quiescent disk with unit optical depth as the environment in which the Uranian satellites accreted. This is very similar to the environment in which the inner Saturnian satellites formed with the exception that in this case accretion began immediately after formation of Uranus, with the full complement of silicates in place (recall that the inner Saturnian satellites were delayed until the region inside of $8R_S$ cooled sufficiently for water condensation). The sole exception to this argument appears to be Miranda, which may have formed close enough to Uranus that water condensation required the planet to cool down (here again the silicates may have been lost in the interim). If this interpretation proves accurate, the Uranian satellite system should be viewed as an analog of the Saturnian, except that in the inner disk the initial gas density was too low to produce a Titan-like object, and the gas density in the outer disk also failed to form an Iapetus sized body (though presumably there was an outer disk for Uranus as well). Our model would explain the lack of a Callisto-Iapetus analog satellite outside the centrifugal radius of Uranus by noting that for objects smaller than Iapetus, gas drag dominates over tidal torque. Hence, one would not expect such a small object to be left stranded.

On the other hand, we interpret the lack of any Uranian satellites close to the centrifugal radius in the inner disk as suggestive of significant satellite migration inwards. To further test this hypothesis we check to see whether the Uranian satellites were expected to stall under the scenario described above.

Here, as in the case of Saturn, planetary tides are insufficient to explain the mass to distance relation since the tides are too weak to move objects the size of the outer Uranian satellites to their present distances. Even assuming that the dissipation parameter for Uranus is low enough that if one starts Miranda at the co-rotation radius it would evolve to its present position over the solar system history, only the positions of Miranda and Ariel may be explained in terms of planetary tides. The difficulty lies not only in explaining the positions of the other satellites, but also why no small satellites are found far from the planet. Given that the centrifugal radius determines the size of the inner gas disk for Uranus, as we have suggested is the general case, one also needs to explain why there are no satellites in the region between $57R_U$ and $22R_U$. We believe that the reason for this is that the Uranian satellites migrated significant distances before they found a radius at which the feedback reaction of the disk stalled their progress. In **Figure 8**, we plot the inertial mass as a function of distance for an inviscid model in which the gas surface density is held constant, and the temperature is fixed at the background temperature of the solar nebula at the position of Uranus for a density of $\rho_s = 1.5$ g cm^{-3}. As we did for the inner Saturnian satellites, the masses of the the Uranian satellites have been corrected to take into account their actual density (see equation 28, and Table II), which affects the amount of gas drag. This curve fits the locations of the Uranian satellites fairly well. Here again, Miranda's location is likely to have been significantly affected by tides. On the other end, according to this criterion Oberon is slightly too far out for its mass. Though the fit is clearly not as good here as it was for the inner Saturnian satellites, we believe it is significant. The more so because the parameters used to obtain the fit are consistent with the scenario used for Saturn and with a minimum mass subnebula.

It must be stressed that in this case the moons are not well separated. Since the separation between Oberon and Titania on the one hand and Umbriel and Ariel on the other is smaller than the damping length for density waves, it would not be valid to assume that each satellite only alters the gas surface density in its own neighborhood. This blurs the meaning of the inertial mass curve to some degree. We would interpret this result to mean that, although slightly less massive than their close neighbors, Oberon and Umbriel originated outside the orbits of Titania and Ariel respectively. In such a situation it might be possible to find a combined equilibrium location such that both satellites change the surface density in their neighborhood. Other possible outcomes include "horse-shoeing", such that the outer, smaller satellite bypasses its inner neighbor and moves inside its orbit (though the chances of this may be small they are not negligible; see Paper I), and resonant capture of the outer body by the inner body (which may apply to Io and Europa, and perhaps Ariel and Umbriel [Tittemore and Wisdom 1988]). It is also possible that the position of satellites was disrupted by collisional events taking place after gas dissipation. Given that several outcomes are possible, one might expect significant scatter in the mass to distance plot. Nevertheless, we find the evidence for such a correlation compelling.

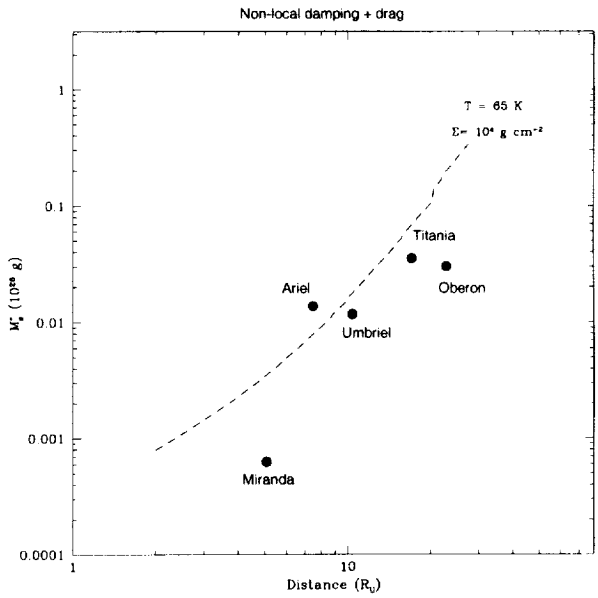

Figure 8: Inviscid inertial mass calculations for $\rho_s = 1.5$ g cm^{-3} for the Uranian system for a constant temperature and gas surface density model using non-local damping and effects due to gas drag. Note that $\Sigma = 10^4$ g cm^{-2} corresponds to gas optical depth of $\tau \sim 1$. The masses of Miranda, and Ariel have been corrected to take into account their actual densities.

7 Conclusions

It is true, of course, that a very long list of caveats can be assembled. However, for the sake of clarity and specificity we have decided to use a consistent model for the regular satellites of Jupiter, Saturn and Uranus. In setting values for the disk properties and in looking for parallels among the various "families" of objects, we have been guided above all by the Hill radius of the primary. The model we have advanced in this study can draw useful parallels between satellite systems. Our model places special emphasis on three distinct locations in the satellite systems. The size of the subnebula disk is placed at $\sim R_H/5$ near the location of the innermost irregular satellites of Jupiter and Saturn. Physically this size is tied to the torque of the Sun on gas flowing from the Roche-lobe into the disk. Closer in at $\sim R_H/48$ the gas density of disk becomes sufficiently high to give rise to large satellites. This location is set by the specific angular momentum of a parcel of gas flowing into the disk. Closer still at $\sim R_H/100$ it is possible to form and stall midsize satellites. For Saturn this radius is determined by the location of water condensation following its accretion. We believe it is essential to explain why it is that at this location Jupiter's Io is ice-free ($\rho_s = 3.53$ g cm^{-3}), Saturn's Rhea is mostly ice ($\rho_s = 1.24$ g cm^{-3}), and Uranus' Oberon is made of ice/rock ($\rho_s = 1.63$ g cm^{-3}).

7 CONCLUSIONS

We investigate a model for giant planet regular satellite formation in which the satellites accrete in the presence of dense inner gaseous disk extending out to the planet's centrifugal radius, and from an extended, low density disk out to a fraction of the planetary Hill radius. We assume a "minimum mass" model to determine the mass of the inner disk. Though there are reasons why significant deviations from this model are possible, we find the predictions of such a model in fair accord with the observations, with the possible exception that the gas density may be a bit high for the satellites to stall at the end of their accretion, even allowing for turbulent removal of gas as the satellites form, so long as the damping of pressure waves is non-local. Hence we are led to consider enhanced concentration of solids by a factor $3-4$ (which may be enough to allow satellites to survive).

Given our subnebula parameters, we show that while protosatellites migrated mostly inwards, it is possible for sizeable objects located in a limited range of radii outside the centrifugal radius to migrate outwards due to the gas tidal torque. While the size of this region is somewhat dependent on the size of the transition region between the inner and outer disks, Saturn's is more extended (out to $\sim 3r_c^S$) compared to Jupiter's (out to $\sim 2r_c^J$) mostly because of Saturn's less massive outer disk and larger Hill radius. Such a region of outward evolution may explain how one can form and then strand satellites as far from the planet as Callisto and Iapetus are found to be.

Survival timescales for satellites in an optically thick giant planet subnebula may be short compared to the lifetime of the subnebula. It might be hoped that satellites would open a gap in the subnebula, but satellites whose Hill spheres are smaller than the scale-height of the subnebula H may not open a gap (Lin and Papaloizou 1993). Because objects can open a gap several times their Roche-lobes, we view the above condition as a loose criterion. Even so, only Ganymede and Titan may have been sufficiently massive to satisfy this constraint. If so, their present locations may reflect the position of the embryos that led to their formation. We would expect nearly all other objects to have undergone significant migration over their history.

To make progress we need to characterize the viscosity properties of the subnebula. As in discussed in Paper I, we expect regions of the disk with temperature close to the background temperature of the nebula at the location of the primary should be nearly quiescent, with low gas viscosity and long evolution times. Because the inner disk of the giant planets (except perhaps Uranus) is non-isothermal both radially and vertically, weak turbulence ($\alpha \sim 10^{-5} - 10^{-6}$) is expected there for as long as the gas remains optically thick (with $\Sigma > 10^4$ g cm^{-2}) given gas opacity only. This assumes that micron-sized dust coagulates quickly and that the equilibrium surface density of such dust gives a dust opacity < 1 everywhere in the disk, at least after satellite accretion has taken place (see Paper I). However, the possibility cannot be ruled out that close to the planet hypervelocity impacts keep the dust opacity high. If so, close to the planet, where dust production is high and the temperature gradient strong, it may be possible to maintain gas turbulence long enough for viscosity to dissipate the inner gas disk on a timescale $10^4 - 10^5$ years, similar to the orbital decay time of Saturn's midsize inner satellites $200 - 700$ km (Titan has an orbital decay timescale ~ 100 years due to the tidal torque, while Iapetus has an orbital decay time in excess of 10^6 years); thus, these midsize satellites may have been left stranded, with the smaller satellites perhaps closer to the planet due to their shorter migration times (although, because in this size range the orbital decay time may not be a monotonic function of size, it is unclear if this mechanism can account for the observed mass versus distance distribution of object). While possible, such a mechanism depends on fine tuning unknown parameters. We look instead for a more general mechanism that does not rely on dust opacity to keep the gas disk optically thick. Nevertheless, we allow for the possibility that not all regular satellites survived for the same reason.

For a satellite to survive in the absence of turbulence the timescale of satellite migration must be longer than the timescale for gas dissipation due to photodissociation or solar wind in $\sim 10^7$ years. For large satellites ~ 1000 km migration is dominated by the gas torque. We derive a new inertial mass criterion and find that the feedback reaction of the gas disk caused by the redistribution of gas surface density around satellites with masses larger than the inertial mass (Ward 1997) can cause a large drop in the drift velocity of such objects, thus making it possible that satellites will be left stranded following gas dissipation. Unlike viscous damping and radial non-linear shock dissipation, vertical wave refraction in the optically thick subnebula and non-linear dissipation at the disk surface (Lin and Papaloizou 1993) may satisfy this requirement. As a simple prescription, we damp the pressure wave a distance $x_{damp} = r_L/m$ from the location from which it was launched. This satisfies the model requirement that the angular momentum the satellite transfers at resonance locations with wavenumber $m \sim r/H$ be deposited in a lengthscale $\sim H$, where most of the torque is exerted. We modify the inertial mass criterion of Ward (1997) in the inviscid limit to include both gas drag, and m-dependent non-local deposition of angular momentum. We use this model to explain the survival of satellites, the mass versus distance relationship apparent in the Saturnian and Uranian satellite systems, and the observation that the inner Saturnian satellites are icy whereas the inner Jovian satellites are rocky. In particular, we argue that planetary tides cannot be responsible for the observed mass to distance relationship of the inner satellites of Saturn and Uranus. The challenge lies not only in explaining the present location of these satellites, but also why there are no small satellites far from the planet. That is, while planetary tides may explain why Mimas, Miranda, and Ariel are not located closer to the planet this mechanism cannot explain why these satellites are not found further out than they are observed to be.

A picture emerges from our model in which some satellites completed their accretion as the subnebula gas optical depth approached unity, while others began their formation in such an environment. This may not be a coincidence to the extent that a much thicker disk may lead to turbulence which keeps the disk warm and prevents condensation. This is significant because when optical depth ~ 1 is reached, the turbulence in the disk

should die down significantly, supporting our assumption that satellites will stall when their mass approaches the *inviscid* inertial mass. Because the inertial mass increases with radial location, even in the case of an optically thick inner disk with a strong temperature gradient and decreasing surface density, we show it is possible for a large object like Ganymede to stall in the outer portion of the inner disk while a smaller one like Io continues to evolve inward until it stalls closer to the planet. At least in the case of Jupiter, in order for this to happen our model appears to require that the subnebula turbulence remove a significant amount of gas on the timescale of satellite accretion (possibly even if an increased solid concentration is favored). On the other hand, it is also possible that wave damping may have been more effective in Jupiter's disk due to the higher optical depth and stronger temperature gradient. If so, the local damping inertial mass curves may be more applicable to Jupiter's satellite system than to that of Saturn.

In this model, the initial gas surface density and the strength of the turbulence are both critical parameters. Though Saturn probably started with $\sim$ 3.7 times less gas in the inner disk that Jupiter, its weaker temperature gradient may mean that the subnebula turbulence was weaker. Thus, in Saturn's case, we argue that either the gas density remained too high for too long to allow rocky satellites inside of Titan to stall and survive, or its satellite embryos formed too slowly to survive bombardment deep in the planetary potential well (though other scenarios, such as a stronger disk feedback reaction in the case of Jupiter, are also possible). Both of these scenarios benefit from the smaller embryo sizes characteristic of Saturn's gas disk.

However, not all the material inside of Titan was lost to the planet. Regions of the disk inside of Rhea initially had a temperature $>$ 250 K, which prevented water condensation. We expect that by the end of Titan's accretion, the inner disk gas density approached the optically thin value. As the planet cooled, the water began to condense in those regions whose initial temperature was previously too high. At that time, the subnebula had already lost most of its silicates by gas drag. Thus, the satellites inside of Titan were formed mostly out of water. We show that when non-local wave damping and gas drag are included, the modified inviscid inertial masses provide a very good fit for the masses of these satellites as a function of position (except that of Mimas and Enceladus whose positions may have been affected by tides or hypervelocity collisions) for a constant density, optically thin disk $\Sigma \sim 10^4$ g cm^{-2} with constant temperature $\sim$ 90 K. This may indicate that although these satellites formed in a warmer environment ($\sim$ 250 K) they continued to slowly migrate inwards as the planet cooled. If so, the present positions of these satellites would reflect their resting place after the planet cooled. For this model to be consistent it requires that the pressure waves damp less efficiently as the planet cools.

A nearly constant temperature and constant surface density model turns out to be important because such a model produces a much steeper slope in the inertial mass versus distance curves. The reason for this is that in the constant temperature case the back-reaction of the disk to the presence of a satellite increases closer to the planet as the decrease in the scale-height of the subnebula allows a greater number of resonances to contribute to the tidal torque. Since the inertial mass is proportional to the surface density, a constant surface density also contributes to make the slope steeper. Given the locations of midsized satellites in Saturn, we expect that the feedback reaction of its inner disk allows such satellites to stall and survive long enough for gas dissipation to take place. On the other hand, Jupiter may not have such satellites because it may not have cooled fast enough to allow for this possibility. It is also possible (though probably unlikely) that the turbulence works in such a way as to remove more gas close to the planet, eventually leading to a disk with zero radial pressure gradient and no gas drag (which would tend to favor survival of small objects close to the planet).

Though subject to significant theoretical uncertainty, the wave damping length we have used is consistent with the separation of the inner satellites of Saturn, such that each satellite is surrounded by its own gas disk reshaped in such a way as to produce a feedback reaction that opposes its inward migration. It might be argued that such a mechanism can only produce a distance to mass relationship if the smaller moons form further out than the larger moons in the first place. However, there are several possible mechanisms that can re-order the moons, such as "horse-shoeing", such that the outer, smaller satellites moves past its inner neighbor, and coalescing of two moons when the disk is still hot followed by relocation when the disk cools. Clearly, though, given our general scenario there are several possible outcomes and a strict mass versus distance relationship may be unlikely. For one thing, collisional events taking place after gas dissipation may alter the positions of the moons. Other possible outcomes may include resonant capture of the outer moon by the inner, larger moon, and combined equilibrium locations for paired moons (outcomes which we speculate may correspond to the satellite system's of Jupiter and Uranus respectively). Instead, one might be led to expect a significant amount of scatter in a satellite mass versus distance plot. Even so, we find the evidence for a mass versus distance correlation of the moons of Saturn and Uranus to be compelling.

Finally, we extend this model to the satellites of Uranus. Though for Uranus the mass of the outer or inner disks may not have been enough to form a Titan or an Iapetus, we find significant similarities between the Uranian satellite system and the Saturnian inner satellites. Our model has both these sets of satellites forming in a cold subnebula with gas optical depth of order unity. In the case of Uranus, a constant density $\sim 10^4$ g cm^{-2} with constant temperature of $\sim$ 68 K inviscid inertial mass model provides a fair fit to the masses of the Uranian satellites as a function of position. However, the main difference with Saturn seems to be that the Uranian satellites have their full complement of silicates in place. This is likely to mean that whereas the Saturnian inner satellites began to form only after the inner disk became cool enough for water condensation, the Uranian satellites began to accrete immediately following planetary accretion (with the possible

exception of Miranda).

We believe that our model manages to incorporate the regular satellites of Jupiter, Saturn and Uranus into the same general scheme. Our model accounts for the wide variation in the distance in Hill radii of the outermost satellite of the three giant planets in a systematic fashion (Oberon is at $\sim 0.4 r_c^U$, Iapetus is at $\sim 3 r_c^S$, Callisto is at $\sim 2 r_c^J$). In the case of Jupiter and Saturn it does so by the outer location of zero tidal torque. Ultimately, the angular momentum in Callisto and Iapetus comes from the torque of the Sun on the gas that flows into the giant planet from its Roche-lobe. For Uranus, the resulting object would be too small for the tidal torque to dominate gas drag, so one would not expect a regular satellite to be left stranded outside the centrifugal radius (this jibes with the presence of Caliban and Stephano, inclined, irregular satellites, at $\sim R_H/10$). Inside the centrifugal radius, our model for the formation of the large, regular satellites indicates that Saturn's satellite system should be viewed as bridging the gap between those of Jupiter and Uranus by combining the formation of a Galilean-sized satellite in an optically thick subnebula with a strong temperature gradient, and the formation of smaller, regular satellites, closer in to the planet, in a cool and nearly constant temperature disk with gas optical depth of order unity.

A moderate $3-4$ increase in the concentration of solids in the subnebula disks relative to solar mixtures (as one may expect from the high-Z content of their parent planets) may improve the chances of satellite survival by decreasing the amount of gas present and allowing for stronger post-accretion gas turbulence for a given temperature profile, lengthen the timescale of formation for Callisto (with smaller embryo sizes), as well as speed up disk cooling after planetary accretion.

ACKNOWLEDGEMENTS

We would like to thank Jeffrey Cuzzi for numerous discussions and for reading the manuscript and suggesting improvements. We also thank Dave Stevenson for discussions. This research was supported by the NRC and a grant from the Planetary Geology and Geophysics program.

References

ARTYMOWICZ, P. 1993. On the wave excitation and a generalized torque formula for Lindblad resonances excited by external potential. *Astrophys. J.* **419**, 155-165.

GOLDREICH, P. AND S. TREMAINE 1980. Disk-satellite interactions. *Astrophys. J.* **241**, 425-441.

GREENBERG, R., D. R. DAVIS, W. K. HARTMANN, AND C. R. CHAPMAN 1977. Size distribution of particles in planetary rings. *Icarus* **30**, 769-779.

HOURIGAN, K., AND W. R. WARD 1984. Radial migration of preplanetary material: Implications for the accretion time scale problem. *Icarus* **60**, 29-39.

LEE, M. H., AND S. J. PEALE 2000. Making Hyperion. Presented at the 32^{nd} DPS meeting, American Astronomical Society, October 2000.

LIN, D. N. C., J. PAPALOIZOU, AND G. SAVONIJE 1990A. Wave propagation in gaseous accretion disks. *Astrophys. J.* **364**, 326-334.

LIN, D. N. C., J. PAPALOIZOU, AND G. SAVONIJE 1990B. Propagation of tidal disturbance in gaseous accretion disks. *Astrophys. J.* **365**, 748-756.

LIN, D. N. C., AND J. PAPALOIZOU 1993. On the tidal interaction between protostellar disks and companions. In *Protostars and Planets III* (E. H. Levy and J. I. Lunine Eds.), pp. 749-836. Univ. of Arizona, Tucson.

LUBOW, S. H., AND F. H. SHU 1975. Gas dynamics of semi-detached binaries. *Astrophys. J.* **198**, 383-405.

LUBOW, S. H., M. SEIBERT, AND P. ARTYMOWICZ 1999. Disk accretion onto high-mass planets. *Astrophys. J.* **526**, 1001.

LYNDEN-BELL, D. AND J. E. PRINGLE 1974. The evolution of viscous disks and the origin of the nebula variables. *Mon. Not. Roy. Astron. Soc.* **168**, 603-637.

POLLACK, J. B., BURNS, J. A., AND TAUBER, M. E. 1979. Gas drag in primordial circumplanetary envelopes: A mechanism for satellite capture. *Icarus* **37**, 587-611.

POLLACK, J. B., A. S. GROSSMAN, R. MOORE, AND H. C. GRABOSKE, JR. 1976. The formation of Saturn's satellites and rings as influenced by Saturn's contraction history. *Icarus* **29**, 35-48.

SAHA, P., AND S. TREMAINE 1983. The orbits of the retrograde Jovian satellites. *Icarus* **106**, 549.

STEVENSON, D. J., A. W. HARRIS, AND J. I. LUNINE 1986. Origins of satellites. In *Satellites* (J. A. Burns and M. S. Matthews, Eds.) Univ. of Arizona Press, Tucson.

TANAKA, H., AND W. R. WARD 2000. Propagation of density waves in a three-dimensional isothermal nebular disk. Presented at the 32^{nd} DPS meeting, American Astronomical Society, October 2000.

TITTEMORE, W. C., AND J. WISDOM 1988. Tidal evolution of the Uranian satellites. I. Passage of Ariel and Umbriel through the 5:3 mean-motion commensurability. *Icarus* **74**, 172-230.

WARD, W. R. 1997. Protoplanet migration by nebula tides. *Icarus* **126**, 261-281.

WARD, W. R., AND K. HOURIGAN 1989. Orbital

migration of protoplanets: The initial limit. *Astrophys. J.* **347**, 490-495.

WARD, 1986. Density Waves in the Solar Nebula: Differential Lindblad Torque. *Icarus* **67**, 164-180.

WEIDENSCHILLING, S. 1984. Evolution of grains in a turbulent solar nebula. *Icarus* **60**, 553-567.

WEIDENSCHILLING, S. 1988. Formation processes and timescales for meteorite parent bodies. In *Meteorites and the Early Solar System* (J. F. Kerridge and M. S. Matthews, Eds.) Univ. of Arizona Press, Tucson.